Journal of Ocean Engineering and Science 10 (2025) 295–307

Contents lists available at ScienceDirect

Journal of Ocean Engineering and Science

journal homepage: www.elsevier.com/locate/joes

Research Paper

Numerical study of the flow at a vertical pile with net-like scour protection matt

Minxi Zhang[a,b], Hanyan Zhao[c], Dongliang Zhao[d], Shaolin Yue[e], Huan Zhou[e], Xudong Zhao[a], Carlo Gualtieri[f], Guoliang Yu[a,b,*]

[a] SKLOE, School of Naval Architecture, Ocean & Civil Engineering, Shanghai Jiao Tong University, Shanghai 200240, China
[b] KLMIES, MOE, School of Naval Architecture, Ocean & Civil Engineering, Shanghai Jiao Tong University, Shanghai 200240, China
[c] Guangdong Research Institute of Water Resources and Hydropower, Guangzhou 510610, China
[d] CCCC Second Harbor Engineering Co., Ltd., Wuhan 430040, China
[e] CCCC Road & Bridge Special Engineering Co., Ltd, Wuhan 430071, China
[f] Department of Structures for Engineering and Architecture, University of Naples Federico II, Italy

ARTICLE INFO

Article history:
Received 27 March 2023
Revised 25 June 2023
Accepted 25 June 2023
Available online 28 June 2023

Keywords:
Numerical simulation
Pile foundation
Local scour
Protective measure
Net-like matt

ABSTRACT

Local scour at a pile or pier in current or wave environments threats the safety of the upper structure all over the world. The application of a net-like matt as a scour protection cover at the pile or pier was proposed. The matt weakens and diffuses the flow in the local scour pit and thus reduces local scour while enhances sediment deposition. Numerical simulations were carried out to investigate the flow at the pile covered by the matt. The simulation results were used to optimize the thickness d_t ($2.6d_{95} \sim 17.9d_{95}$) and opening size d_n ($7.7d_{95} \sim 28.2d_{95}$) of the matt. It was found that the matt significantly reduced the local velocity and dissipated the vortex at the pile, substantially reduced the extent of local scour. The smaller the opening size of the matt, the more effective was the flow diffusion at the bed, and smaller bed shear stress was observed at the pile. For the flow conditions considered in this study, a matt with a relative thickness of $T = 7.7$ and relative opening size of $S = 7.7$ could be effective in scour protection.

1. Introduction

Piles are typically used as the supporting pillar for bridges, wharfs, offshore platforms, and offshore wind turbines. The piles sit on the bed and their presence modify the flow patterns in the immediate vicinity and may cause increased local sediment transport and local scouring. Such scour could have adverse impact on the stability of these piles. Due to large damages related to pile scour failure in China [1–3] and elsewhere [4–6], the research on possible protective measures for local scour at piles is of great significance.

The literature about the fundaments of local scour at piles or piers is extensive [3,7–11]. Local scour at pile is mainly caused by three flow features: downflow in front of pile, horseshoe vortex around pile and wake vortex at the lee of pile [12–14]. It is known well that the strength of downflow needs to be weakened to reduce the local scour at pile [15,16].

A scour protection measure should serve two goals [17]. The first goal is to increase the erosion resistance of the sediment bed. This is considered as a passive approach, usually achieved by placing a protective layer of coarse granular materials, riprap, or concrete blocks at the base of the pier [18–25]. The second goal is to weaken the downflow and horseshoe vortex. This active approach, which is also termed as flow-altering countermeasure, is usually achieved by placing an extended base plate, apron, sacrificial piles, or collar at or around the pile [26–30]. Engineering practices have already shown that the passive approach, although flexible and can be applied readily, often needs regular repair and maintenance at the later stage. The active approach is usually expensive, has limited application, and is difficult to install. Tafarojnoruz et al. [31] compared six different types of flow-altering countermeasures (submerged vanes, bed sill, transverse sacrificial piles, collar, threading, and pier slot) against pier scour and found that some of these measures, despite having been recommended as highly efficient in the literature, did not perform well under different test conditions. The efficiency associated with bed sill, submerged vanes, and threading was found to be lower than 20%, whereas using collar, pier slot, and transverse sacrificial piles were

* Corresponding author at: SKLOE, School of Naval Architecture, Ocean & Civil Engineering, Shanghai Jiao Tong University, Shanghai 200240, China.
E-mail address: yugl@sjtu.edu.cn (G. Yu).

https://doi.org/10.1016/j.joes.2023.06.002

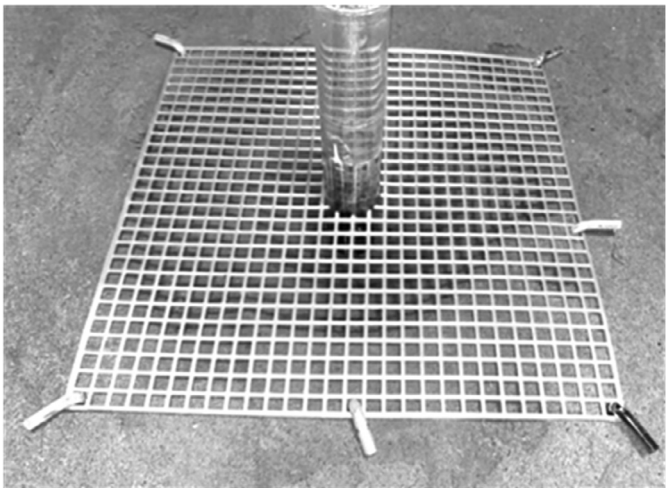

Fig. 1. Protection matt over the scour pit.

found to reduce the maximum scour depth by approximately 35% or lower.

Recently, a scour protection approach which produces increased local resistance and sediment deposition has emerged. This approach uses bed protection devices and includes tetrahedral permeable frames [32], triangular structures [33], artificial grass [34], and floating curtains [35]. This approach not only reduces bed scour but also increases sediment deposition. However, the approach has certain shortcomings. For example, the triangular structures [33] and artificial plants [36] are not suitable for bed experiencing high flow velocity. Furthermore, planting may be considered the invasion of foreign species [37], and the vegetation is also limited by its own growth cycle and environment [38]. The floating curtains are not suitable where there are changes in the flow direction [36]. Hence, more effective countermeasures against local scour at piles in rivers and oceans are still needed.

This study proposes the application of a net-like matt as a protection against local scour at pile. Such matt is in the form of a flexible net with certain thickness, rigidity, and pore opening, and is made of corrosion and UV-resistant polymers, such as HDPE with a specific weight slightly larger than 1.0. The matt can be placed to cover the potential scour pit location using a supporting frame, and anchored with self-penetration torpedo anchors [39,40]. It is expected that the matt could significantly reduce the downflow and could also trap sediment particles at the openings. While the matt does not reduce the approach flow strength and bedload transport rate, the matt with its geometrical features, such as the matt thickness and opening size, would significantly affect the flow field at the pile. In this study, numerical simulations were conducted to investigate the flow characteristics at the net-like matt structure placed over and fully covering the scour pit formed below. The effects of the matt thickness and opening size on flow velocity, turbulent kinetic energy, and bed shear stress inside the scour pit were studied and discussed.

2. The hydrodynamic model

Figs. 1 and 2 show the matt and side view of the layout of the matt, where the h_0 is the equilibrium scour depth at the pile without the protection matt. The numerical model was set up to include the upstream and downstream flat bed and flow boundaries, free surface, and fully developed scour pit. This was the base model. Then, the scour protection matts of various thicknesses and opening sizes were incorporated, and the flow field at the matt and inside the scour pit were simulated. In this way, the changes in the flow field and turbulence level within the pit could be obtained.

2.1. Governing equations of numerical model

Numerical simulations were conducted using commercial software Flow-3D. The flow is described using the Reynolds-averaged Navier-Stokes (RANS) equations and represents the conservation of mass and momentum for an incompressible viscous fluid as follows:

Continuity equation:

$$\frac{\partial}{\partial x_i}(u_i A_i) = 0 \tag{1}$$

Momentum equation:

$$\frac{\partial u_i}{\partial t} + \frac{1}{V_F}\left(u_i A_i \frac{\partial u_i}{\partial x_j}\right) = -\frac{1}{\rho}\frac{\partial p}{\partial x_i} + G_i + f_i \tag{2}$$

in which, x_i and x_j are Cartesian coordinates; u_i is the time-averaged velocity component in x, y, and z directions, respectively; p is the time-averaged pressure; A_i is the area fraction of the fluid in the i direction; t is the time; V_F is the volume fraction of the fluid part; ρ is the fluid density; G_i is the gravitational acceleration in the i direction; f_i is the viscous force acceleration in the i direction.

Following Gumgum and Guney the RNG κ-ε turbulence model was used in this study to simulate the flow around and inside the scour pit [41]. In the model, the κ equation and ε equation are, respectively:

$$\frac{\partial(\rho k)}{\partial t} + \frac{\partial(\rho k u_i)}{\partial x_i} = \frac{\partial}{\partial x_j}\left[\alpha_k(\mu + \mu_t)\frac{\partial k}{\partial x_j}\right] + G_k - \rho\varepsilon \tag{3}$$

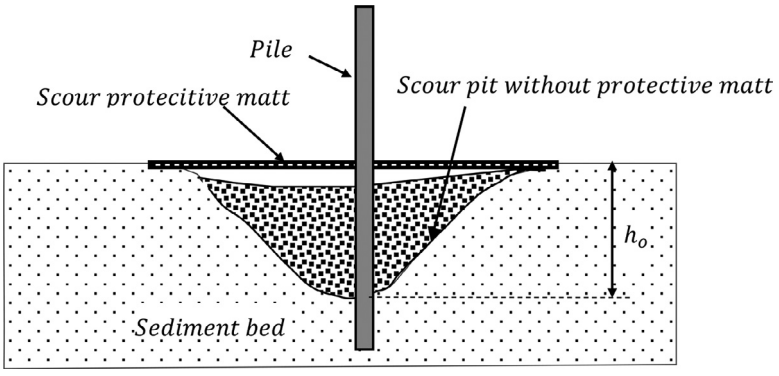

Fig. 2. Local scour pit of pile below the protection matt.

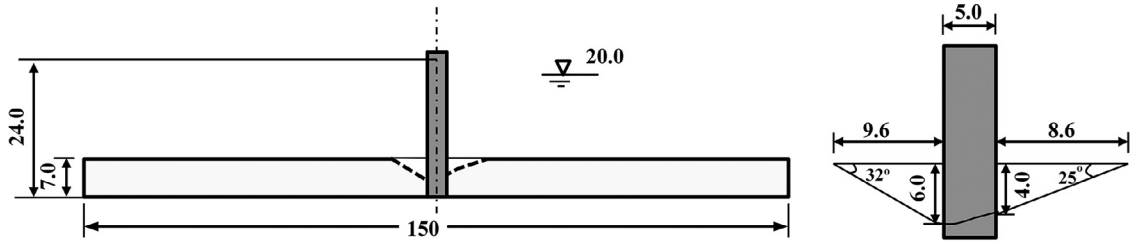

(a) Simulation domain of the numerical model (b) Pile in pre-molded scour pit

Fig. 3. Layout of pile and pre-molded scour pit in the numerical model (unit in cm).

Table 1
Numerical test conditions; pile diameter, D = 5 cm; flow depth, h = 20 cm; approach velocity, $\boldsymbol{v_a}$ = 38 cm/s.

Runs	Relative opening size $S = d_t/d_{95}$	Relative thickness $T=d_t/d_{95}$	Scour depth, h_p (cm)
1	∞	0	6.0
2	7.7	7.7	6.0
3	12.8	2.6	6.0
4	12.8	7.7	6.0
5	12.8	12.8	6.0
6	12.8	17.9	6.0
7	17.9	7.7	6.0
8	23.1	7.7	6.0
9	28.2	7.7	6.0

$$\frac{\partial(\rho\varepsilon)}{\partial t}+\frac{\partial(\rho\varepsilon u_i)}{\partial x_i}=\frac{\partial}{\partial x_j}\left[\alpha_\varepsilon(\mu+\mu_t)\frac{\partial\varepsilon}{\partial x_j}\right]+C_{1\varepsilon}^{*}\frac{\varepsilon}{k}G_k-\rho C_{2\varepsilon}\frac{\varepsilon^2}{k} \tag{4}$$

where κ is the turbulent kinetic energy; ε is the turbulent energy dissipation rate; μ is the dynamic viscosity; μ_t is the turbulent dynamic viscosity, and G_k is the turbulent kinetic energy generated by the time-averaged velocity gradient, $C_{\varepsilon1}^{*}=C_{\varepsilon1}-\frac{\eta(-\frac{\eta}{\eta_0})}{1+\beta\eta^2}$, $C_{\varepsilon1}=1.42$, $\eta=(2E_{ij}\cdot E_{ij})^{1/2}\frac{k}{\varepsilon}$, $E_{ij}=\frac{1}{2}(\frac{\partial u_i}{\partial x_j}+\frac{\partial u_j}{\partial x_i})$, $\eta_0=4.377$, $\beta=0.012$, $C_{\varepsilon2}=1.68$

2.2. Layout of numerical model

In the numerical model, the reported scour pit measured during the flume experiments in Zhao et al. (2022) [42] was applied for the numerical model. The pile diameter was 5 cm. The maximum scour depth in front of the pile was 6 cm and the depth at the lee of the pile was 4 cm (Fig. 3). The depth-averaged approach velocity and water depth were 0.38 m/s and 0.20 m, respectively. The pore openings of the matt were square, and the relative opening size $S = d_n$ /d_{95} was 7.7, 12.8, 17.9, 23.1, and 28.2, respectively, where d_n is the opening size of the matt and d_{95} is the grain diameter of the sediments in Zhao et al. (2022) such that 95% of diameters are finer. The relative matt thickness $T = d_t$ /d_{95} was 2.56, 7.7, 12.8, and 17.9, respectively, where d_t is the thickness of the matt. The conditions used for the numerical simulations are listed in Table 1. The numerical domain was reduced to 1.50 m (L) × 0.50 m (W) × 0.24 m (H) to save on computational resources.

2.3. Mesh generation and boundary conditions

Structured orthogonal mesh was adopted for mesh generation, and different sizes of mesh were tested to obtain a convergent solution [43,44]. The size of the mesh was initially set to be 8 mm × 8 mm × 8 mm. To accurately capture the geometry and the hydrodynamics features around the matt opening and the scour pit, the mesh size was reduced to 1.8 mm × 1.8 mm × 1.8 mm as shown in Figs. 4 and 5. The total number of cells was about 2.66 million. To ensure the stability of the calculation, the starting time step was set to 0.01 s, and the minimum time step was set to 10^{-8} s. The dimensionless coordinate along the flow direction is defined as X = x/L, the dimensionless coordinate of the lateral axis is defined as Y= y/W, and the dimensionless coordinate perpendicular to the bed is defined as Z= z/h.

At the upstream boundary, the inflow velocity was specified, and a pressure boundary condition was applied for the downstream and top boundaries to achieve a uniform flow. At the bed, pile, and matt, a no-slip boundary condition was applied. The sidewall boundaries were set as symmetry boundary conditions, where no fluid is exchanged and no energy transfers through.

2.4. Model validation

With the matt covering the scour pit, the flow field inside the scour pit is not available. Thus, only the experimental results of depth-average flow velocity near the pile and over the matt reported in Zhao [45] were used to validate the numerical model. The comparisons of the measured and simulated data are shown in Figs. 6 and 7, where the subscript S represents the simulated data, the subscript M represents the measured data, L_1 is the longitudinal extent and L_2 is the transverse extent. It is noted that the numerical model accurately simulated the velocity distribution in front of and at the lee of the pile along the streamwise direction, but slightly over predicted the velocity at the side of the pile. The relative errors between the numerical simulation and laboratory experiment were less than 10%. The error might be related to the symmetry boundary applied at the sides of the simulation domain.

3. Results and analysis

3.1. Effects of protection matt on the hydrodynamics in the scour pit

(1) Effects on the flow velocity in the scour pit

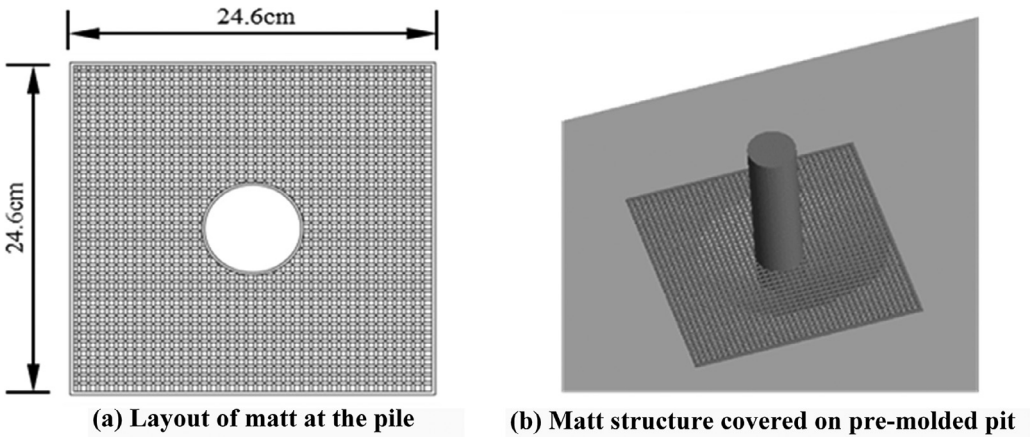

Fig. 4. Matt structure and its layout in the flume.

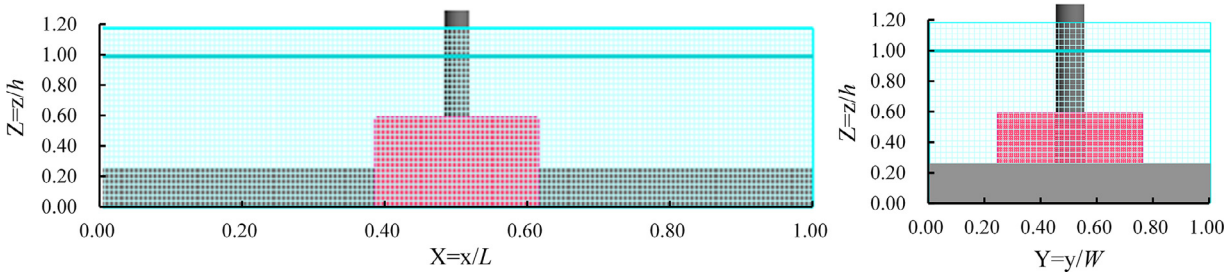

Fig. 5. Mesh of the numerical model.

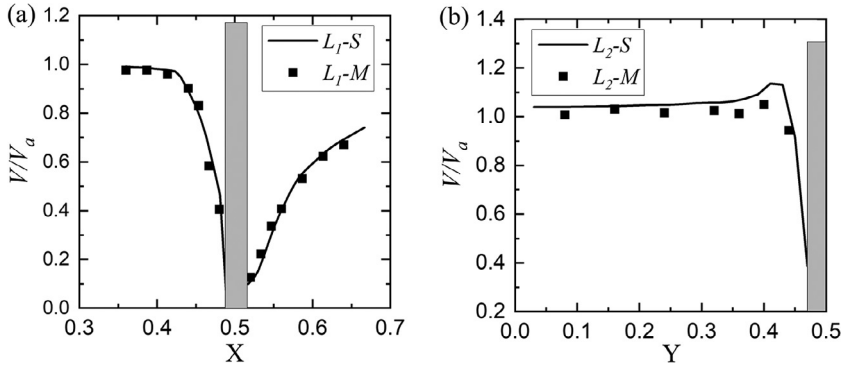

Fig. 6. Comparison of the simulated (Run 1) and experimental results for the depth-average velocity at the center line of the (a) streamwise direction and (b) transverse direction.

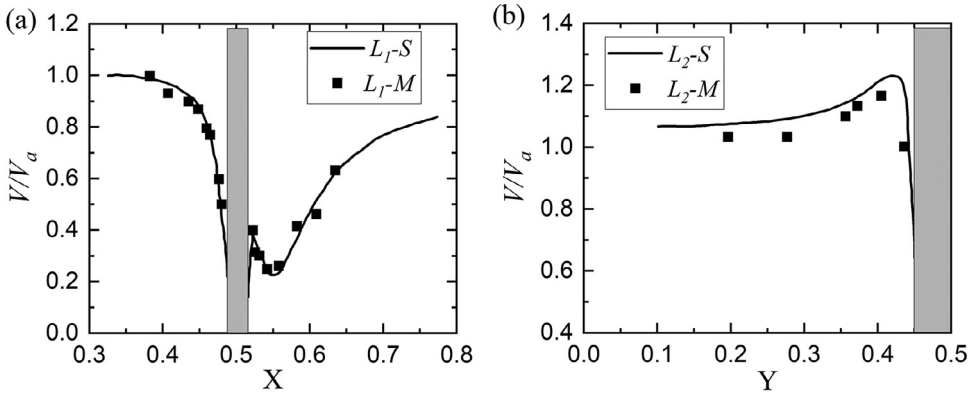

Fig. 7. Comparison of the simulated (Run 2) and experimental results for the depth-average flow velocity over the matt at the center line of the (a) streamwise direction and (b) transverse direction.

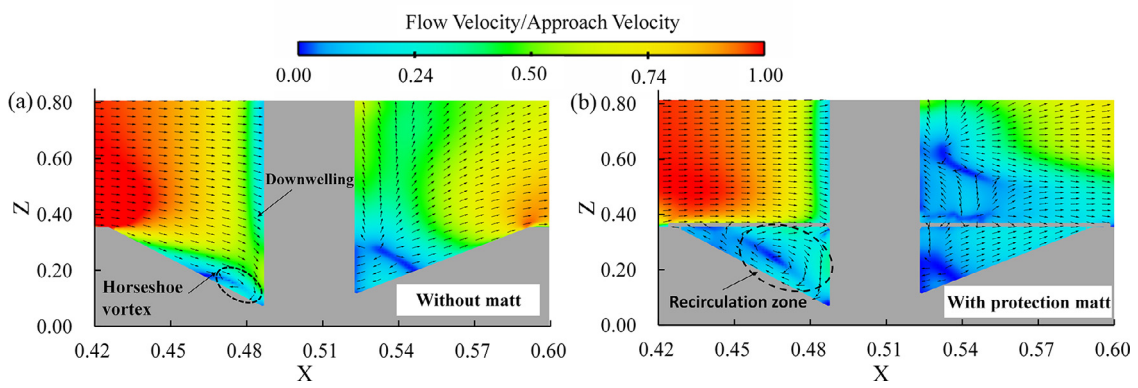

Fig. 8. Distribution of flow velocity on the x-z plane ($Y = 0.5$) (a) Run 1 without and (b) Run 2 with the protection matt.

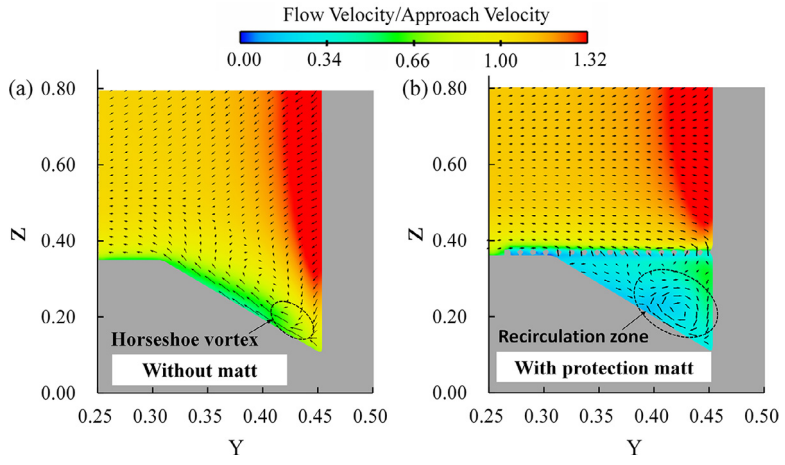

Fig. 9. Distribution of flow velocity on the y-z plane ($X = 0.5$) (a) Run 1 without and (b) Run 2 with the protection matt.

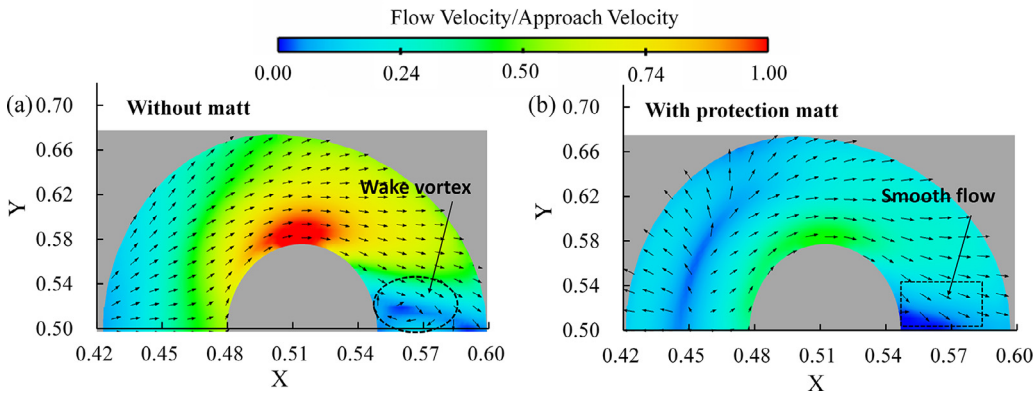

Fig. 10. Distribution of flow velocity on the x-y plane ($Z = 0.175$) (a) Run 1 without and (b) Run 2 with the protection matt.

Figs. 8–10 show a comparison of the velocity distribution at the pile with and without the matt (Runs 1 and 2). The matt had significantly reduced the magnitude of flow velocity in the scour pit. Without the matt, the downwelling flow converged with the approaching flow in front of the pile forming a vortex near the pile (Figs. 8 and 9). The downwelling flow was blocked by the matt and the near-bed horseshoe vortices with relatively high velocity ($\approx 0.3v_a \sim 0.5v_a$ in front of the pile and $0.5v_a \sim 1.1v_a$ at the pile side) created large recirculation zones with low velocity (less than $0.1v_a$ in front of the pile and $0.3v_a$ at the pile side) for almost 80% and 70% of the scour pit area in front of and at the side of the pile, respectively. Such recirculation zones might lead to trapping and deposition of sediment around the pile.

One may also observe that, with the matt, the flow velocity in the scour pit at the side of the pile decreased by 300% (from more than $0.8v_a$ to lower than $0.3v_a$), and that at the lee of the pile reduced to almost 0 m/s (Fig. 10). In other words, the flow became relatively stagnant, and the wake vortex disappeared.

(2) Effects on the turbulent kinetic energy in the scour pit

Local scour is caused by the eroding forces of flow acting on the erodible bed in the vicinity of the pile. Besides the mean flow features, turbulence fluctuation also exerts a strong influence during the scouring process. Here, the turbulent kinetic energy in the scour pit was analyzed as this parameter is relevant to the sedi-

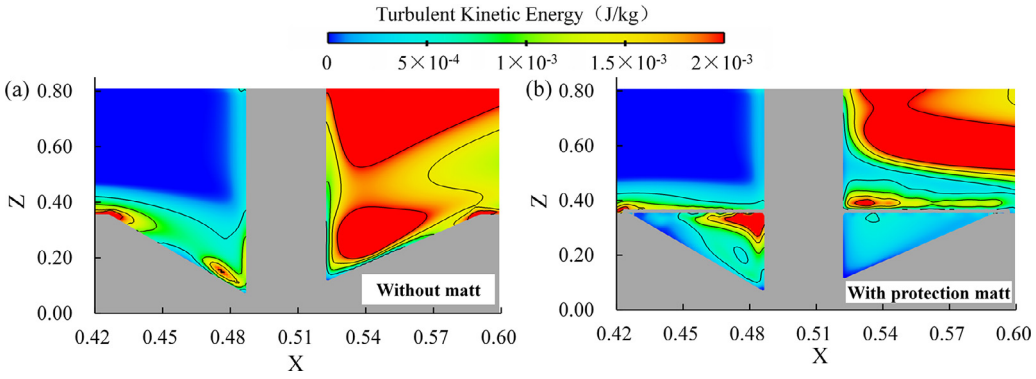

Fig. 11. Distribution of turbulent kinetic energy on the x-z plane ($Y = 0.5$) (a) without and (b) with the protection matt.

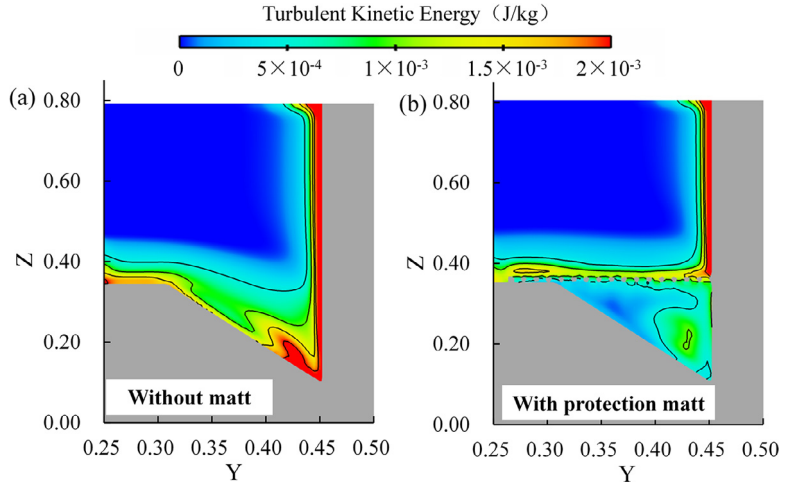

Fig. 12. Distribution of turbulent kinetic energy on the y-z plane ($X = 0.5$) (a) without and (b) with the protection matt.

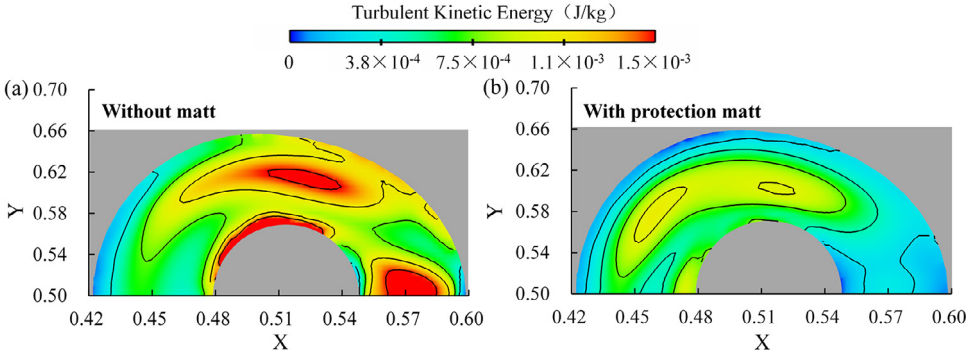

Fig. 13. Distribution of turbulent kinetic energy on the x-z plane ($Z = 0.175$) (a) without and (b) with the protection matt.

ment entrainment, transport, and deposition. The turbulent kinetic energy k is described as follows:

$$k = \frac{\overline{\left(u_i'\right)^2} + \overline{\left(v_i'\right)^2} + \overline{\left(w_i'\right)^2}}{2} \tag{5}$$

where $\overline{(u_i')^2}$, $\overline{(v_i')^2}$, and $\overline{(w_i')^2}$ are the mean square values of the longitudinal, transverse, and vertical fluctuating velocity components, respectively.

Figs. 11–13 show the comparison of the turbulent kinetic energy distribution on the x-z, y-z, and x-y planes around the pile with and without the protection matt, respectively. Clearly, the matt significantly weakened the kinetic energy inside the scour pit. Fig. 11 shows the turbulent kinetic energy on the x-z plane ($Y = 0.5$) with and without the matt. Without the matt, the core regions of the turbulences in front of the pile were located close to the bottom of the scour pit where the turbulent kinetic energies were larger than 2.0×10^{-3} J/kg, and the k-value was particularly large behind the pile. With the matt, the k-value in the scour pit at the lee of the pile was greatly reduced to about 2×10^{-4} J/kg which was an order of magnitude lower than that without the matt. The core region of the turbulences in front of the pile had moved to the position below the matt nearer to the pile. The near bed k-value was about 6×10^{-4} J/kg which was 70% lower compared with the case without the matt. The effect of flow turbulence at the bottom of the scour pit would be small. The distribution of the turbulence kinetic energy in the y-z plane and x-y plane are presented in Figs. 12 and 13, respectively. These figures

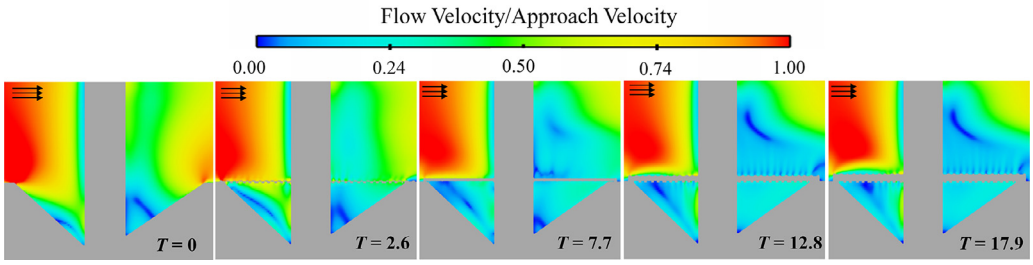

Fig. 14. Distribution of flow velocity on the x-z plane ($Y = 0.5$) for various T-values.

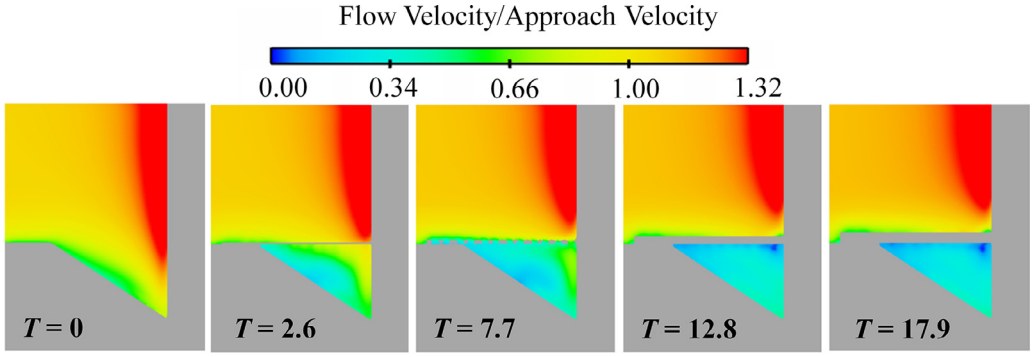

Fig. 15. Distribution of flow velocity on the y-z plane ($X = 0.5$) for various T-values.

show that the k-value in the scour pit at the pile side was reduced by more than 50% with the matt cover. This observation indicated that without the protection matt, the flow energy was expended in scouring the bed and finally dissipated at the bottom of the scour pit, and the turbulences at the bottom were violent. With the protection matt, however, the flow energy was mainly dissipated at the matt, and the turbulence near the bed surface in the scour pit was very much weaker in comparison. Thus, one may conclude that significant scour under the matt would not be observed.

3.2. Effects of matt thickness on the hydrodynamics in the scour pit

Theoretically, as the matt thickness increases, the structural strength, cost as well as the corresponding flow diffusion should be larger. However, the matt thickness also affects the formation of secondary scour under the matt. Thus, matt thickness should be optimized. The following discussions are based on Run 1 (without matt) and Run 3, 4, 5, and 6 (with matt for various thicknesses) where the relative opening size S was held constant at 12.8 to analyze the influence of the matt thickness on the flow patterns in the scour pit.

(1) Effects of matt thickness on the flow velocity in the scour pit

Figs. 14 and 15 show the velocity distribution on the x-z plane ($Y = 0.5$) and y-z plane ($X = 0.5$) with the matt for various relative thicknesses $T = 0$ (without the matt), 2.6, 7.7, 12.8, and 17.9, respectively. The longitudinal and transversal distribution of velocity in the scour pit ($Z = 0.2$, 2/3 of the scour pit depth from its bottom) are shown in Figs. 16 and 17, respectively.

As the matt thickness increased, the velocity in the scour pit decreased. For $T = 2.6$, the flow velocity near the bottom surface of the matt in front of the pile was larger than $0.5v_a$ which was at least 4 times higher than that for $T = 7.7$, 12.8, and 17.9. Near the upper surface of the matt, the velocity at the lee of the pile for $T = 2.6$ was still larger than $0.5v_a$ which was close to that without the matt. The flow velocity for $T = 7.7$, 12.8, and 17.9 decreased dramatically by 75% and which was less than $0.1v_a$ (Fig. 14), indicating that the sediment may be prone to be deposited at the lee of the pile. The difference in velocity between the cases with $T = 12.8$ and 17.9 was small (Fig. 15).

The matt significantly reduced the horizontal velocity in the scour pit in front of and at the side of the pile (Figs. 16 and 17). Compared with the case without protection matt (Run 1), when the scour pit was covered by the protection matt with $T = 7.7$ (Run 4), the horizontal velocity in the scour pit in front of the pile decreased from $0.3v_a$ (without matt) to almost 0 (with matt), and that at the side of pile decreased by 75% (from $0.5v_a$ to $0.1v_a$). However, the matt appeared to have little effect on the vertical velocity at the front and side of the pile but showed a relatively larger effect on the vertical velocity at the lee of the pile. Without the matt (Run 1), the direction of vertical flow velocity u_z in front of the pile and at the lee of the pile was downward, and the largest u_z in front of the pile was $0.6v_a$. For $T = 7.7$ (Run 4), the largest u_z in front of the pile was decreased by 34% to $0.4v_a$, and that at the lee of the pile was close to 0 (Fig. 16(b)).

(2) Effects of matt thickness on the turbulent kinetic energy in the scour pit

In terms of turbulent kinetic energy, the matt with various thicknesses had a different degree of shadowing effects (Figs. 18 and 19). Above the matt, the horizontal turbulent zone appeared close to the upper surface of the matt in front of the pile, and the zone gradually increased as T increased (Fig. 18). In the scour pit, the turbulent kinetic energy at the lee of the pile decreased as T increased (Fig. 18). However, in front of and at the sides of the pile (Figs. 18 and 19), the turbulent kinetic energy for $T = 2.6$ was even larger than that without the matt. As T increased, the vortex at the side of the pile gradually disappeared. For $T = 7.7$ (Run 4), the near bed turbulent kinetic energy in front of the pile was the least and decreased by more than 75%, and that at the side of the pile decreased by about 50% which showed little difference from those for $T = 12.8$ and $T = 17.9$, respectively.

(3) Effects of matt thickness on the bed shear stress on the scour pit bottom

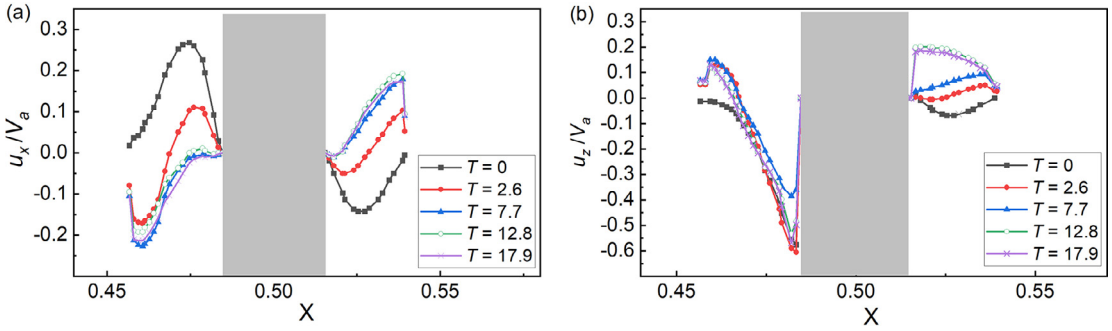

Fig. 16. Longitudinal distribution of (a) horizontal and (b) vertical velocity ($Z = 0.2$) for with various T-values.

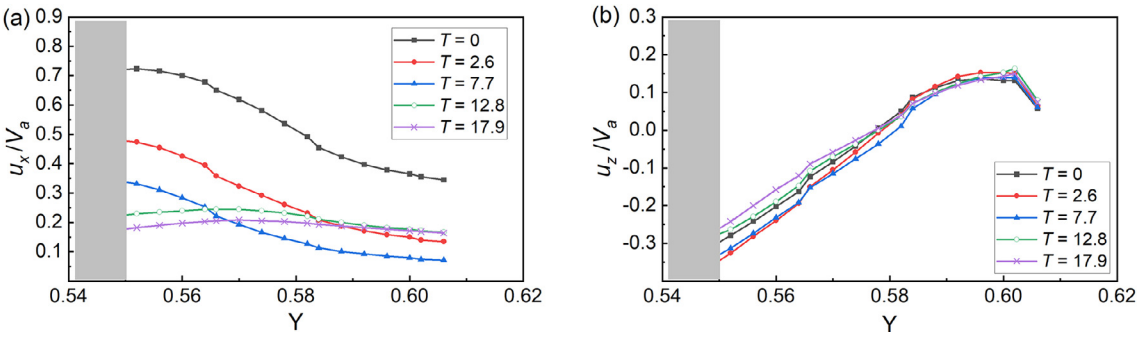

Fig. 17. Transversal distribution of the (a) horizontal and (b) vertical velocity ($Z = 0.2$) for various T-values.

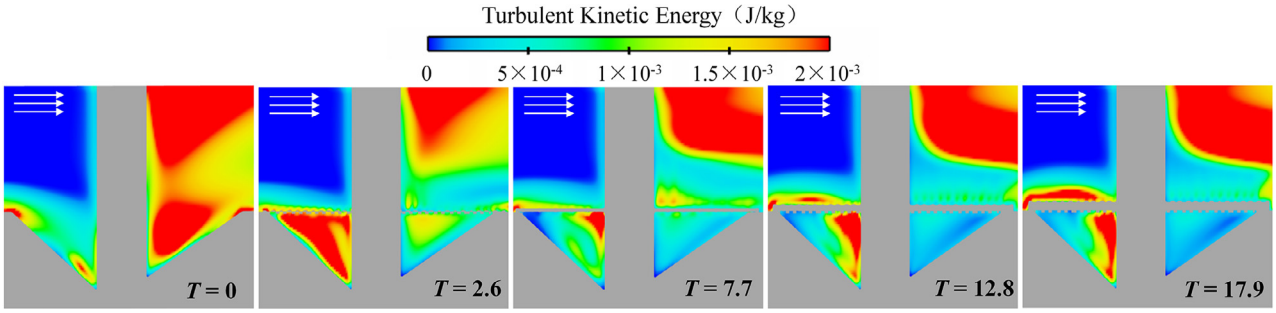

Fig. 18. Distribution of turbulent kinetic energy on the x-z plane ($Y = 0.5$) for different T.

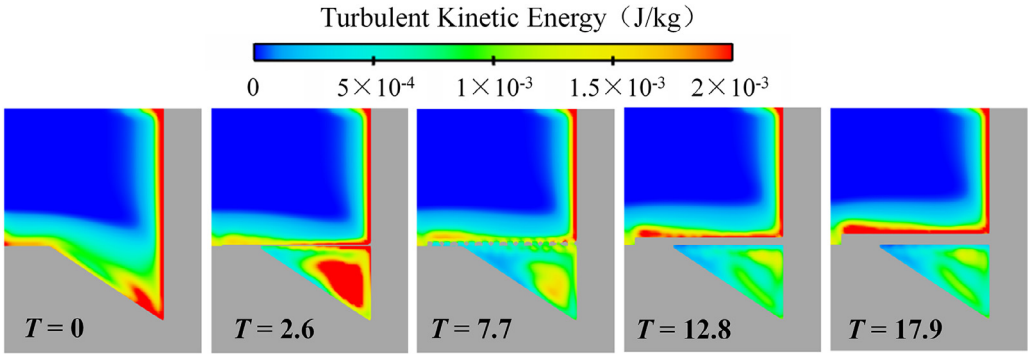

Fig. 19. Distribution of turbulent kinetic energy on the y-z plane ($X = 0.5$) for different T.

The protective effect of matt on local scour was investigated by analyzing the bed shear stress in the scour pit. Eight representative locations at various locations of the scour pit were selected (Fig. 20), in which, p_1, p_2, and p_3 were located in front of the pile along the longitudinal section; p_4 and p_5 were located at the lee of the pile; p_6, p_7, and p_8 were located at the side of the pile.

The relative bed shear stresses (τ/τ_0, where τ is the local bed shear stress with the matt, and τ_0 is that without the matt) at those 8 locations varied with T (Fig. 21). At location p_1, τ was weakened to the largest extent compared to p_2 and p_3, which showed only 3% ~ 17% of τ_0, and T had little effect on τ. At location p_2, τ was higher than τ_0, but τ was very small. At location p_3, τ was lower than τ_0, and it was largest to the greatest extent

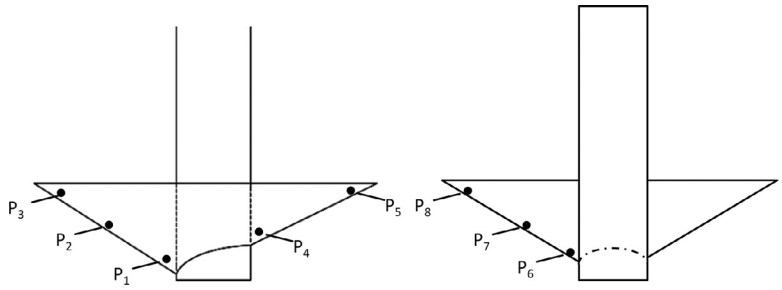

Fig. 20. Point locations for bed shear stress measurement in the scour pit.

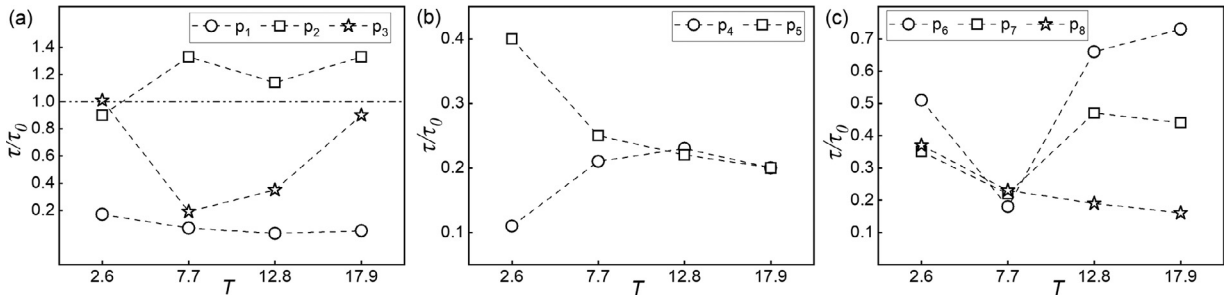

Fig. 21. τ/τ_0 at selected point locations in the scour pit for various T.

for $T = 7.7$, being only 19% of τ_0. At locations p_4 and p_5, τ was reduced by more than 50% with the matt, and the effect of T on the bed shear stress was no longer significant for $T > 7.7$. At locations p_6 and p_7, τ-values were all less than τ_0 and were the least for $T = 7.7$. At location p_8, τ decreased with T, which was 16% ~ 37% of τ_0.

Through the analysis of bed shear stress at the various locations in front of, at the lee, and the side of the pile, one may conclude that the matt thickness has a significant influence on the bed shear stress in the scour pit. In general, when the scour pit was covered by the matt with $T = 7.7$, the bed shear stress in the scour pit would be the least, which was 7~25% of the corresponding τ_0-values without the matt.

By considering the changes of velocity, turbulent kinetic energy, and bed shear stress in the scour pit under the protection matt with various thicknesses, one may conclude that the velocity, turbulent kinetic energy, and bed shear stress in the scour pit were significantly reduced when $T = 7.7$. Therefore, the matt thickness was set as $7.7d_{95}$ in the subsequent evaluation of the matt opening size.

3.3. Effects of matt opening size on the hydrodynamics in the scour pit

The matt opening size would directly affect the through flow characteristics of the matt, and in turn affect the sediment active process in the scour pit. To further explore the effect of the opening size on the hydrodynamics in the scour pit, various matt opening sizes were considered, namely $S = \infty$ (without the matt), 7.7, 12.8, 17.9, 23.1, and 28.2 (Run 2, 4, and 7~9), respectively, while T was held constant at 7.7.

(1) Effects of matt opening size on the flow velocity in the scour pit

It can be seen from Fig. 22 that the matt with $S =$ 7.7~23.1 significantly reduced the flow velocity in the scour pit, and that the overall velocity was less than $0.3v_a$. However, when S was increased to 28.2, the matt protection appeared less effective as the downflow velocity in the scour pit was larger than $0.7v_a$. For $S = 7.7$, the overall flow velocity in the scour pit was the least. Quantitively, it can be seen from Figs. 23 and 24 that the near bed ($Z = 0.2$) horizontal velocity u_x in the scour pit around the pile decreased significantly under the matt. The u_x-value in front of and at the lee of the pile decreased to almost 0, and the largest value of u_x at the side of the pile decreased by about 52%, when the relative opening size was $S = 7.7$ (Run 2). The weakening of the vertical velocity u_z around the pile was not obvious.

(2) Effects of matt opening size on turbulent kinetic energy in the scour pit

Figs. 25 and 26 show the turbulent kinetic energy distribution on the x-z plane ($Y = 0.5$) and y-z plane ($X = 0.5$), respectively, with the matt with $S = \infty$, 7.7, 12.8, 17.9, 23.1, and 28.2. It can be seen from Fig. 25 that the turbulent kinetic energy in the scour pit behind the pile was significantly reduced for any finite S-value, and the near bed turbulent kinetic energy in front of the pile decreased as S decreased. For $S = 28.2$, the value of the near bed turbulent kinetic energy was about 1.9×10^{-3} J/kg which was close to that without the matt (2×10^{-3} J/kg), indicating that the opening size $S = 28.2$ was too large and had a negligible effect on the flow. The core turbulent region in the scour pit at the side of the pile expanded and near the bed the turbulent kinetic energy increased by 400% as S increased from 7.7 to 28.2 (Fig. 26). Within the range of the opening size in the present study, the smaller the opening size, the weaker the turbulence near the bed surface in the scour pit.

(3) Effects of matt opening size on bed shear stress on the scour pit bottom

The results of the bed shear stress (τ) at locations p_1-p_8 in the scour pit under the matt with various opening sizes are listed in Table 2. It can be seen from Fig. 27 that S shows a significant influence on τ around the pile, especially at the side of the pile (p_4 and p_5). At p_1, τ was weakened to the largest extent compared to p_2 and p_3, which were 3% ~ 21% of τ_0; and τ increased with S. At p_2, τ was higher than τ_0 except for $S = 7.7$. At p_3, S showed little effect on the relative bed shear stress, and τ was 18%~34% of τ_0. At p_4 and p_5, the τ-value in the scour

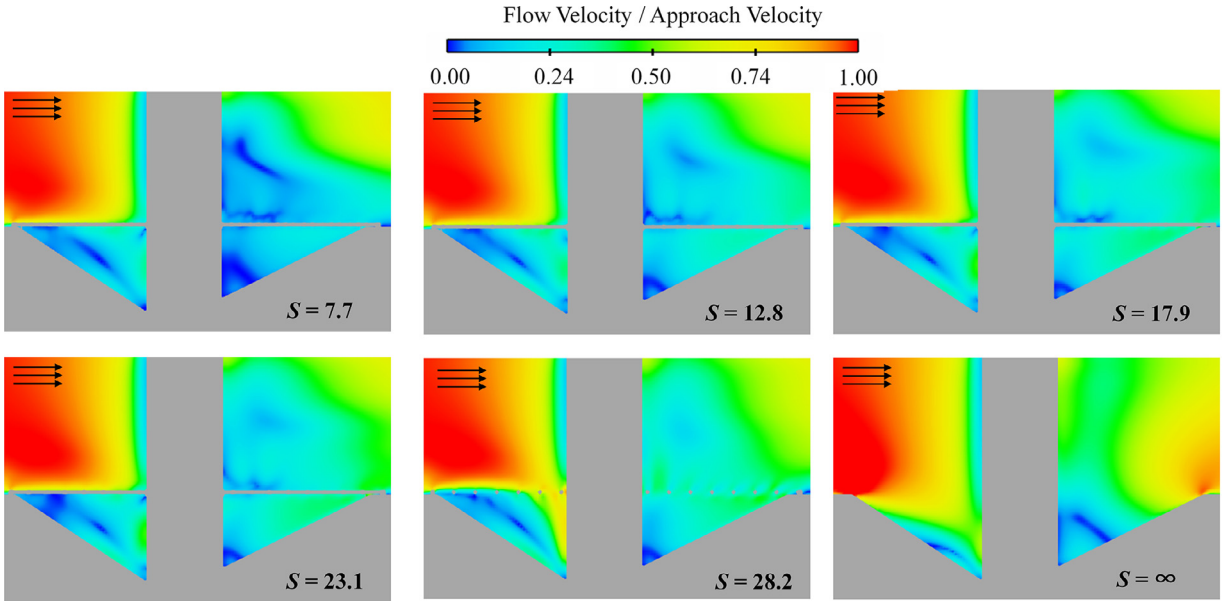

Fig. 22. Distribution of flow velocity on the x-z plane ($Y = 0.5$) for various S.

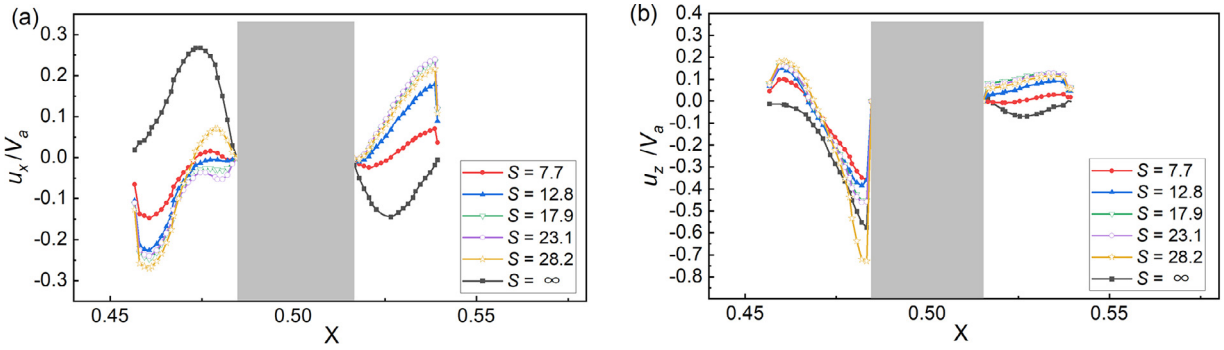

Fig. 23. Longitudinal distribution of the (a) horizontal and (b) vertical velocity ($Z = 0.2$) for various S.

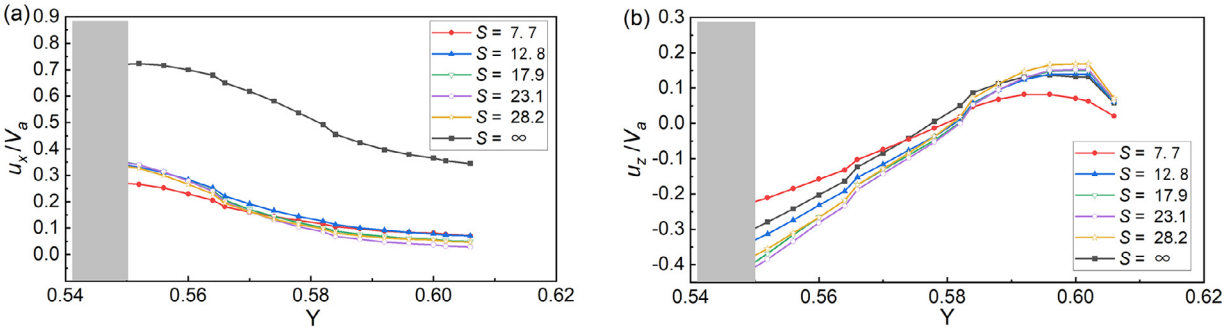

Fig. 24. Transversal distribution of the (a) horizontal and (b) vertical velocity ($Z = 0.2$) for various S.

Table 2
Bed shear stresses in the scour pit for matt with different S.

S	τ (Pa)							
	p_1	p_2	p_3	p_4	p_5	p_6	p_7	p_8
7.7	0.006	0.036	0.007	0.011	0.028	0.014	0.034	0.041
12.8	0.015	0.065	0.006	0.035	0.047	0.014	0.036	0.049
17.9	0.018	0.073	0.007	0.050	0.059	0.035	0.035	0.038
23.1	0.016	0.069	0.006	0.052	0.069	0.033	0.033	0.065
28.2	0.044	0.083	0.011	0.045	0.071	0.044	0.040	0.041
∞	0.210	0.050	0.030	0.160	0.190	0.080	0.160	0.220

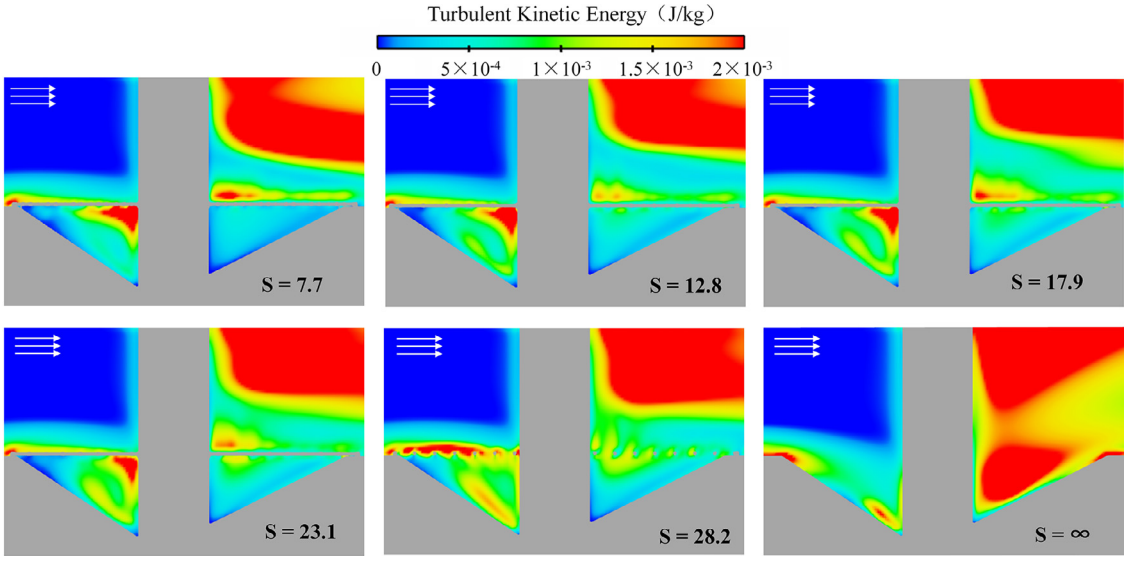

Fig. 25. Distribution of the turbulent kinetic energy on the x-z plane ($Y = 0.5$) for various S.

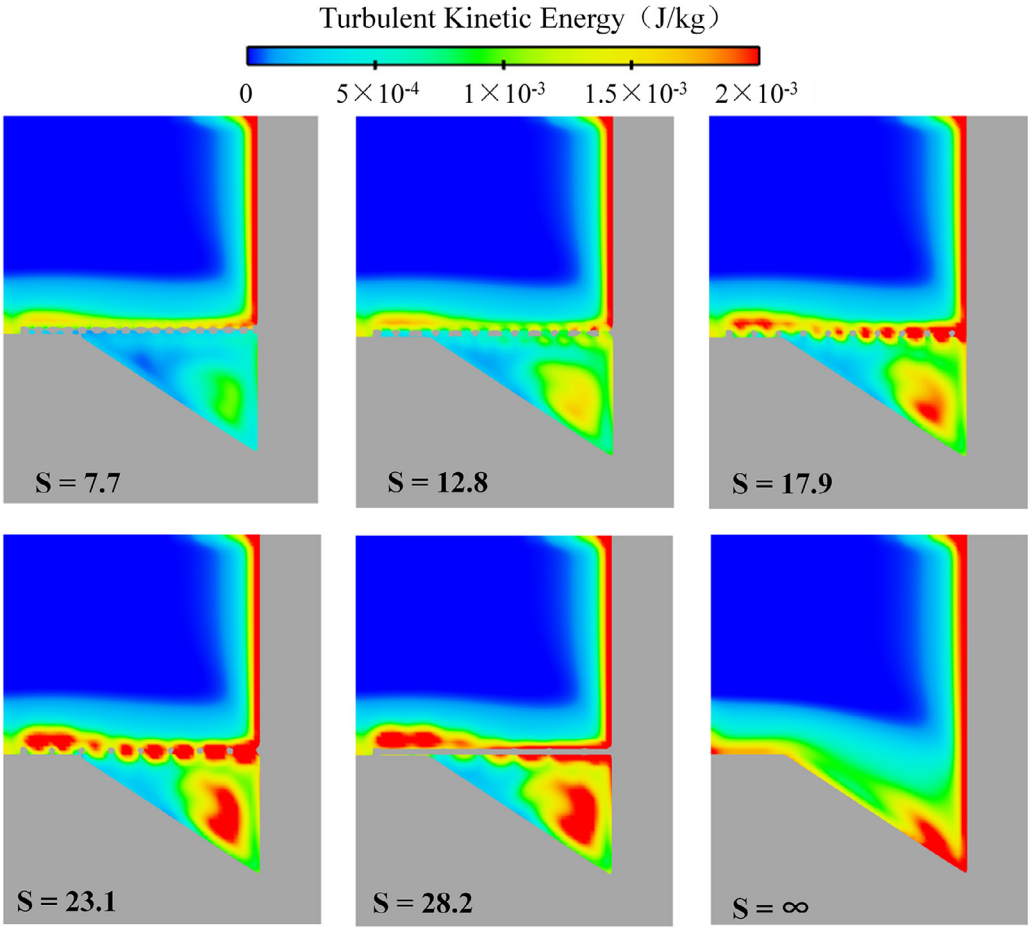

Fig. 26. Distribution of the turbulent kinetic energy on the y-z plane ($X = 0.5$) for various S.

pit was only 7%~37% of τ_0 under the matt, and τ was the least for $S = 7.7$. At p_6, p_7, and p_8, τ was the least for $S = 7.7$, for which τ/τ_0 was 0.19~0.21. As can be seen in Fig. 27(c), the flow blocking effect of the matt was weaker as S was larger than 17.9, as τ/τ_0 at p_6 increased sharply to more than 0.4 and continued to increase sharply. To sum up, the smaller the opening size of the matt, the better the weakening effect on the velocity in the scour pit, and the weaker the scour ability of the flow around the pile.

According to Zhang and Yu [46], for fine sediments, the critical bed shear stress could be as low as 0.11 Pa and increases with the increased grain size. Meanwhile, the critical bed shear stress of cohesive sediments depends on the fluidization degree of sediments, which could be as large as 1.00 Pa and as low as 0.045 Pa.

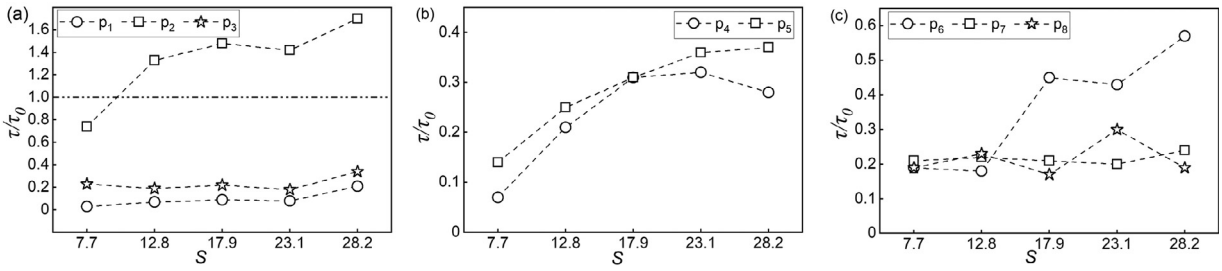

Fig. 27. τ/τ_0 at selected point locations in the scour pit for various S.

The higher the fluidization degree, the smaller the critical bed shear stress, and the easier the sediments would be eroded. In the present study, the bed shear stresses at those eight points were all lower than 0.041 Pa (Table 2) for $S = 7.7$, which means that the bed sediments in the scour pit protected by the matt would not be eroded even if the bed was fully fluidized. Accordingly, one may conclude that the matt with the $S = 7.7$ and $T = 7.7$ could be effective in weakening the hydrodynamics forces in the scour pit and the bed sediments in the scour pit would be protected and not eroded.

4. Discussion

This study considered using a net-like protection matt to reduce the extent of local scour at the pile while enhances sediment deposition in the scour pit. The matt may be placed on the bed during the pile installation or immediately after the pile installation. The matt can significantly weaken the flow strength in the scour pit and reduce the sediment carrying capacity of the flow, so that the local scour at the pile is presumably reduced and the sediment near the pile may be prone to be deposited under the protection of the matt. It is worth noting that the opening size of the matt is very important, and the optimal opening size may vary with flow or sediment conditions. Compared to other values of S in this study, $S = 7.7$ was effective in weakening the flow velocity and hydrodynamics forces in the scour pit. However, the ability of the incoming sediments to fall through the matt openings into the scour pit is constrained by such opening size. A large matt opening may lead to sediments to fall through easily. Since the process of the sediment passing through the matt openings is too complicated to be simulated so far, laboratory experiments should be further carried out to investigate the effectiveness of the matt to reduce the scour and enhance the sediment deposition at the pile. This part will be presented in a future study.

Compared with the past scour protection methods, using the matt poses certain advantages, such as good flow sheltering effects and increased potential sediment deposition. The matt could also be prefabricated on land. However, the matt requires strong and stable anchors at the edges, and a buoyant force to suspend the matt over the scour pit. As the scour pit may be wide, then the span of the matt could be large. Then, the density of the matt material should be as low as possible to reduce the structural weight (submerged weight) under the premise of ensuring the safety of the structure. Ideally, the density of the matt may be close to the water density. On the other hand, it would be difficult to install a large piece of light matt on the scour pit around the pile in the deep-water field due to the disturbances of currents and waves. The structural frames and matt boards may be designed for case by case in engineering practices also considering the financial effort, and the installation and anchorage technologies need further focused study.

5. Conclusions

In this study, the application of a net-like protection matt against local scour at piles was presented. FLOW-3D software was used to numerically investigate the flow velocity, turbulent kinetic energy, and bed shear stress at the pile in uniform steady currents with and without the matt over the scour pit. The influence of the matt thickness and opening size on the flow at the pile was discussed. The conclusions are as follows:

The matt does not change the approach flow velocity and sediment transport ability characteristics beyond the extent of the matt, but significantly reduces the flow velocity inside the scour pit and below the matt. In front of the pile, the downflow passes through the matt and its strength is significantly decreased. The extent of the horseshoe vortex at the pile side and wake vortex at the lee of the pile were both reduced. Instead, large recirculation zones with low flow velocity are observed in front of and at the side of the pile. Such recirculation zones might lead to sediment deposition around the pile.

The matt thickness affects the flow patterns in the scour pit. The velocity, turbulent kinetic energy, and bed shear stress in the scour pit are both reduced significantly for a dimensionless thickness $T = 7.7$. For a dimensionless thickness T lower than 7.7, the effect of matt thickness on hydrodynamics and scour was negligible.

The opening size of the matt also affects the flow patterns in the scour pit. The smaller the opening size, the weaker the flow in the scour pit. The matt with $S = 7.7$ had a great effect in reducing the flow velocity, turbulent kinetic energy, and bed shear stress in the scour pit. However, a large opening may lead sediment to fall through that may be beneficial to the sediment deposition in the scour pit. The optimal matt opening size for the local scour reduction and sediment deposition needs to be further studied through laboratory experiments.

Declaration of Competing Interest

The authors declare that they have no known competing financial interests or personal relationships that could have appeared to influence the work reported in this paper.

CRediT authorship contribution statement

Minxi Zhang: Conceptualization, Methodology, Validation, Formal analysis, Writing – original draft, Visualization. **Hanyan Zhao:** Formal analysis, Investigation. **Dongliang Zhao:** Validation, Resources. **Shaolin Yue:** Methodology, Resources. **Huan Zhou:** Methodology, Resources. **Xudong Zhao:** Investigation. **Carlo Gualtieri:** Writing – review & editing. **Guoliang Yu:** Conceptualization, Resources, Supervision, Project administration, Funding acquisition.

Acknowledgments

This work was financially supported by National Natural Science Foundation of China (No. 52171268) and CCCC Road & Bridge Special Engineering Co., Ltd. The authors are thankful to the anonymous reviewers for their valuable comments and suggestions to improve the quality of the paper.

References

[1] C. He, Mod. Transp. Technol. 17 (3) (2020) 46–59 in Chinese.
[2] X. Wen, D. Zhang, J. Tianjin Univ. 54 (10) (2021) 998–1007 (Science and Technology)in Chinese.
[3] M. Zhang, H. Sun, W. Yao, G. Yu, Ocean Eng. 265 (2020) 112652, doi:10.1016/j.oceaneng.2022.112652.
[4] K. Wardhana, F.C. Hadipriono, J. Perform. Constr. Fac. 17 (3) (2003) 144–150, doi:10.1061/(ASCE)0887-3828(2003)17:3(144).
[5] R. Ettema, G. Constantinescu, B.W. Melville, J. Hydraul. Eng. 143 (9) (2017) 03117006, doi:10.1061/(ASCE)HY.1943-7900.0001330.
[6] C. Valela, C.D. Rennie, I. Nistor, Int. J. Sediment Res. 37 (1) (2021) 37–46, doi:10.1016/j.ijsrc.2021.04.004.
[7] B.W. Melville, A.J. Sutherland, J. Hydraul. Eng. 114 (10) (1988) 1210–1226, doi:10.1061/(ASCE)0733-9429(1988)114:10(1210).
[8] E.V. Richardson, S.R. Davis, Evaluating Scour At Bridges, 4th ed., United States Department of Transportation, Federal Highway Administration, Washington, DC., 2001.
[9] D.M. Sheppard, B. Melville, H. Demir, J. Hydraul. Eng. 140 (1) (2014) 14–23, doi:10.1061/(ASCE)HY.1943-7900.0000800.
[10] A.O. Aksoy, G. Bombar, T. Arkis, M.S. Guney, J. Hydrol. Hydromech. 65 (1) (2017) 26–34.
[11] D.T. Bui, A. Shirzadi, A. Amini, et al., Sustainability 12 (3) (2020) 1063, doi:10.3390/su12031063.
[12] B.M. Sumer, J. Fredsoe, The Mechanics of Scour in Marine Environments. World Advanced Series on Ocean Engineering, 17, World Scientific, Singapore, 2002.
[13] J. Unger, W.H. Hager, Exp. Fluids 42 (1) (2007) 1–19.
[14] G. Kirkil, S.G. Constantinescu, R. Ettema, J. Hydraul. Eng. 134 (5) (2008) 82–84, doi:10.1061/(ASCE)0733-9429(2008)134:5(572).
[15] B. Dargahi, J. Hydraul. Eng. 116 (10) (1990) 1197–1214.
[16] A. Bestawy, T. Eltahawy, A. Alsaluli, M. Alqurashi, Water Supply 20 (3) (2020) 1006–1015, doi:10.2166/ws.2020.022.
[17] Y.M. Chiew, J. Hydraul. Eng. 118 (9) (1992) 1260–1269.
[18] D. Bertoldi, R. Kilgore, in: Hydraulic Engineering '93, ASCE, San Francisco, California, United States, 1993, pp. 1385–1390.
[19] Y.M. Chiew, J. Hydraul. Eng. 121 (9) (1997) 635–642.
[20] C.S. Lauchlan, B.W. Melville, J. Hydraul. Eng. 127 (5) (2001) 412–418, doi:10.1061/(ASCE)0733-9429(2001)127:5(412).
[21] P.F. Lagasse, P.E. Clopper, L.W. Zevenbergen, L.G. Girard, National Cooperative Highway Research Program (NCHRPReport 593), Countermeasures to protect bridge piers from scour, Washington, DC, NCHRP, 2007.
[22] S. Jiang, Z. Zhou, J. Ou, J. Sediment Res. (4) (2013) 63–67 in Chinese.
[23] A. Galan, G. Simarro, G. Sanchez-Serrano, J. Hydraul. Eng. 141 (6) (2015) 06015004, doi:10.1061/(ASCE)HY.1943-7900.0001003.
[24] Z. Zhang, H. Ding, J. Liu, Ocean Eng. 33 (2) (2015) 77–83 in Chinese.
[25] C. Valela, C.N. Whittaker, C.D. Rennie, I. Nistor, B.W. Melville, J. Hydraul. Eng. 148 (3) (2022) 04022002 10.1061/%28ASCE%29HY.1943-7900.0001967.
[26] B.W. Melville, A.C. Hadfield, J. Hydraul. Eng. 6 (2) (1999) 1221–1224, doi:10.1061/(ASCE)0733-9429(1999)125:11(1221).
[27] V. Kumar, K.G. Rangaraju, N. Vittal, J. Hydraul. Eng. 125 (12) (1999) 1302–1305.
[28] A.M. Yasser, K.S. Yasser, M.A. Abdel-Azim, Alex. Eng. J. 54 (2) (2015) 197–203, doi:10.1016/j.aej.2015.03.004.
[29] S. Khaple, P.R. Hanmaiahgari, R. Gaudio, S. Dey, Acta Geophys. 65 (2017) 957–975, doi:10.1007/s11600-017-0084-z.
[30] C. Valela, I. Nistor, C.D. Rennie, in: Proceedings of the 6th International Disaster Mitigation Specialty Conference, Fredericton, Canada, Canadian Society for Civil Engineering, 2018, pp. 235–244.
[31] A. Tafarojnoruz, R. Gaudio, F. Calomino, J. Hydraul. Eng. 138 (3) (2012) 297–305, doi:10.1061/(ASCE)HY.1943-7900.0000512.
[32] H. Tang, S. Fang, Y. Zhou, K. Cai, Y.M. Chiew, S.Y. Lim, N.S. Cheng, in: Proceedings of the 2nd International Conference Scour and Erosion (ICSE-2), Singapore. Singapore, Nanyang Technological University, 2004.
[33] W. Zhang, Y. Li, X. Wang, Z. Sun, J. Sichuan Univ. 06 (2005) 34–40 (Engineering Science Edition)in Chinese.
[34] S. Yang, B. Shi, Trans. Oceanol. Limnol. 5 (2017) 43–47 in Chinese.
[35] H. Wang, F. Si, G. Lou, W. Yang, G. Yu, J. Waterw. Port Coast. Ocean Eng. 141 (1) (2015) 04014030, doi:10.1061/(ASCE)WW.1943-5460.0000270.
[36] L.D. Meyer, S.M. Dabney, W.C. Harmon, Trans. ASAE 38 (3) (1995) 809–815.
[37] G. Spyreas, B.W. Wilm, A.E. Plocher, D.M. Ketzner, J.W. Matthews, J.L. Ellis, E.J. Heske, Biol. Invasions 12 (5) (2010) 1253–1267, doi:10.1007/s10530-009-9544-y.
[38] T. Lambrechts, S. François, S. Lutts, R. Muñoz-Carpena, C.L. Bielders, J. Hydrol. 511 (2014) 800–810, doi:10.1016/j.jhydrol.2014.02.030.
[39] G. Yu, Dynamic Embedded Anchor with High Frequency Micro Amplitude Vibrations. CN patent No: ZL200810038546.0, 2008.
[40] X. Chen, M. Zhang, G. Yu, Ocean Eng. 236 (2021) 109315, doi:10.1016/j.oceaneng.2021.109315.
[41] F. Gumgum, M.S. Guney, in: Proceedings of the 6th International Conference Engineering and Natural Sciences (ICENS), Serbia, Belgrade, 2020.
[42] H. Zhao, S. Yue, H. Zhou, M. Zhang, G. Yu, Ocean Eng. 40 (5) (2022) 111–120 in Chinese.
[43] B. Blocken, C. Gualtieri, Environ. Modell. Softw. 33 (2012) 1–22, doi:10.1016/j.envsoft.2012.02.001.
[44] N.D. Bennett, B.F. Croke, G. Guariso, et al., Modell. Softw. 40 (2013) 1–20, doi:10.1016/j.envsoft.2012.09.011.
[45] X. Zhao, Effectiveness and Mechanism of Lattice On Sedimentation and Anti-Erosion of Local Scour Hole At Piers, Shanghai Jiao Tong University, Shanghai, China, 2023.
[46] M. Zhang, G. Yu, Water Resour. Res. 53 (9) (2017) 7798–7815, doi:10.1002/2017WR021066.